

SHORT COMMUNICATIONS

Acta Cryst. (1995). **D51**, 1065–1070

Crystallization and preliminary X-ray diffraction analysis of double-helical RNA octamers. By MARTIN EGLI* and STEFAN PORTMANN, *Organic Chemistry Laboratory, ETH Swiss Federal Institute of Technology, CH-8092 Zürich, Switzerland*, and DANUTA TRACZ, CHRISTOPHER WORKMAN and NASSIM USMAN, *Ribozyme Pharmaceuticals Inc., 2950 Wilderness Place, Boulder, CO 80301, USA*

(Received 28 December 1994; accepted 15 March 1995)

Abstract

Single crystals of a chemically synthesized self-complementary RNA octamer with sequence r(CCCCGGGG) have been obtained by screening 50 different conditions at room temperature using a standard sparse-matrix sampling method. Two crystal forms with different morphologies grew under diverse crystallization conditions within days by hanging-drop vapor diffusion. Hexagonal crystals with space group $P6_122$ (one strand per asymmetric unit) and unit-cell dimensions $a = b = 39.73$ and $c = 58.55$ Å diffracted to 2.6 Å. Rhombohedral crystals with space group $R32$ (one duplex per asymmetric unit) and unit-cell dimensions $a = b = 42.38$ and $c = 131.70$ Å (hexagonal setting) diffracted beyond 1.5 Å. Data sets for both crystal forms were collected on image-plate/rotating-anode generator equipment and structure determinations and refinements are under way.

Introduction

To date only very few RNA oligonucleotides have been crystallized, and in all cases the resolutions obtained were lower than 2 Å. The fragments investigated include duplexes with standard Watson–Crick type base pairs (Dock-Bregeon *et al.*, 1988; Lorenz *et al.*, 1993), and duplexes comprising GU wobble base pairs (Holbrook, Cheong, Tinoco & Kim, 1991; Cruse *et al.*, 1994), as well as GA mismatches (Leonard *et al.*, 1994) and UU mismatches (Baeyens, De Bondt & Holbrook, 1995). Structure determinations of transfer RNA's (Kim *et al.*, 1973; Robertus *et al.*, 1974; Moras *et al.*, 1980), tRNA–synthetase complexes (Rould, Perona, Söll & Steitz, 1989; Ruff *et al.*, 1991; Biou, Yaremchuk, Tukalo & Cusack, 1994), RNA viruses (Fisher & Johnson, 1993; Larson *et al.*, 1993), a bacteriophage coat protein–operator complex (Valegård, Murray, Stockley, Stonehouse & Liljas, 1994), a spliceosomal protein complexed with an RNA hairpin (Oubridge, Ito, Evans, Teo & Nagai, 1994), as well as a hammerhead ribozyme (Pley, Flaherty & McKay, 1994) have yielded additional information on RNA tertiary structure. However, RNA fine structure, ion coordination and hydration, among others, have been investigated only to a limited extent, and more high-resolution structures are thus needed. DNA chemical synthesis is well established and numerous X-ray crystallographic studies of oligodeoxynucleotides have provided detailed insight into the polymorphic nature of DNA structure (Kennard & Hunter, 1991; Dickerson, 1992; Joshua-Tor & Sussman, 1993; Egli, 1994). Compared with DNA, chemical synthesis of RNA is considerably more difficult, so far resulting in limited amounts of pure material for

structural work. Recently improved and perfected protection and purification protocols can now yield oligoribonucleotides in quantities and quality suitable for crystallization experiments (Scaringe, Francklyn & Usman, 1990; Usman, Egli & Rich, 1992; Wincott *et al.*, 1995).

We selected two octameric sequences, r(CCCCGGGG) and r(GGGCGCCC), for chemical synthesis and X-ray crystallographic analysis. The choice was based on the fact that these sequences had previously been crystallized as the corresponding DNA oligonucleotides. In both cases, the duplexes adopted A-type conformations (Haran, Shakked, Wang & Rich, 1987; Rabinovich, Haran, Eisenstein & Shakked, 1988), and in the case of the d(GGGCGCCC) octamer, the availability of two crystal forms provided clues about the influence of crystal packing on DNA conformation (Shakked, Guerstein-Guzikevich, Eisenstein, Frolov & Rabinovich, 1989). A-DNA and A-RNA double helices bear close structural resemblance, and it was hoped that the two oligonucleotides might crystallize more readily than others. We report here, in a preliminary fashion, the crystallization and structural analysis for two crystal forms of r(CCCCGGGG), and crystallization experiments for r(GGGCGCCC).

Results and discussion

Synthesis and purification

The two octamers were synthesized on an ABI 390Z large-scale DNA/RNA synthesizer in a 25 µmol scale, according to described procedures (Scaringe *et al.*, 1990; Usman *et al.*, 1992) with cycle and deprotection modifications to accommodate the larger scale of synthesis (Wincott *et al.*, 1995). The fully deprotected oligomers were then purified by anion-exchange chromatography on a Pharmacia fast protein liquid chromatography using an anion-exchange Mono Q, HR-16 (20 ml), column and a gradient consisting of 10–150 mM NaClO₄. The appropriate fractions were pooled and desalted on reversed phase C-18 Sep-Pak (Waters) media. The eluants were evaporated to dryness to yield white powders (~60% overall yield). Denaturing polyacrylamide gel electrophoresis showed a single band and analytical ion-exchange high-pressure liquid chromatography showed a single peak in both cases.

Crystallization

Initial crystallization trials for r(CCCCGGGG) used the sitting-drop vapor-diffusion method with well established components for nucleic acid fragment crystal growth, such as cacodylate buffer, magnesium chloride, spermine-tetrahydrochloride and 2-methyl-2,4-pentanediol (MPD) precipitant. Droplets of 20 µl containing 1.3 mM RNA, 16–25 mM sodium cacodylate pH 6.9, 2–5 mM MgCl₂ and 1–1.5 mM

* Author to whom correspondence should be addressed.

spermine-tetrahydrochloride, were equilibrated against 25 ml MPD [35%(v/v)], resulting in long brittle needles that were typically twinned and diffracted only to relatively low resolution. To search for improved crystallization conditions, a total of 50 conditions, based on the sparse-matrix approach by Jancarik & Kim (1991), were screened with the standard hanging-drop technique (Crystal Screen, Hampton Research). In the individual chambers, droplets consisting of 5 μ l well solution and 5 μ l RNA solution (2.1 mM) were equilibrated against 0.5 ml well solution. Several conditions produced crystals, whereby two crystal forms were observed, and the results are summarized in Table 1. Micrographs of selected hexagonal and rhombohedral crystals are depicted in Fig. 1.

The two crystal forms grow over a remarkably wide range of conditions, however, in both cases there are well components that seem of particular importance for crystallization. Rhombohedral crystals grow from solutions with pH between 4.6 (Na acetate, condition 47) and 8.5 (Tris-HCl, condition 4), but the most perfect crystals were obtained from solutions containing ammonium sulfate as the precipitant (conditions 4, 39 and 47, Table 1). Rhombohedral crystals resulted in the absence of ammonium sulfate as well (condition 26, Fig. 1, Table 1), but these crystals were more sensitive compared with those grown under the above conditions and cracks due to rapid solvent loss appeared on their surface already during mounting. In addition, an examination of the crystals that were initially obtained with the sitting-drop technique showed them to be isomorphous with the rhombohedral form. Similarly, the two conditions resulting in reasonably well diffracting hexagonal crystals are supplemented with CaCl₂ (condition 1 and 24, Table 1). However, the optimal pH range seems to be much more narrow compared with the rhombohedral form (the buffer in both cases is Na acetate pH 4.6 and the only difference between the two media is the nature of the precipitant, 2-methyl-2,4-pentanediol *versus* isopropanol). For the hexagonal crystal form, condition No. 1 was refined and large crystals of typical size 0.7 \times 0.4 \times 0.4 mm appeared after two weeks in droplets consisting of 1 mM RNA, 50 mM Na cacodylate pH 4.5, 7.8 mM CaCl₂, equilibrated against a reservoir of 30% MPD.

A similar approach was used for the crystallization of the octamer r(GGGCGCCC). In general crystals of this sequence were of poorer quality and in many cases resembled the needles that were initially obtained in the sitting-drop experiments with the r(CCCCGGGG) octamer. No crystals of the hexagonal type were observed in general.

Data collection and preliminary structural analysis

Cell constants and space groups of some of the crystals shown in Table 1 were determined from precession photographs and diffractometer measurements. Rhombohedral crystals are of space group *R*32 and hexagonal crystals are of space group *P*6₁22/*P*6₅22. Data for a hexagonal crystal grown under refined conditions No. 1 and a rhombohedral crystal grown under conditions No. 47 were collected on an MAR research image-plate system (300 mm diameter), mounted on an Enraf-Nonius rotating-anode generator FR 591 (λ Cu *K* α = 1.5418 Å). The cell constants of the hexagonal crystals are $a = b = 39.73$ and $c = 58.55$ Å. The crystal-to-detector distance was 150 mm and a total of 182 frames with a frame size of 0.5° were collected. The resulting 18 505 reflections were merged to 2034 unique reflections with an overall merge factor of 4%. Data are

Table 1. Sparse-matrix conditions (Jancarik & Kim, 1991) resulting in r(CCCCGGGG) crystals

Crystalline material was also observed under additional conditions, but the crystal systems could not be determined either optically or from precession photographs and diffractometer measurements.

Condition No.	Crystal form	Time	Remarks
1*	Hexagonal	2 weeks	Smooth edges, 2 vertexes along hexagonal direction
4*	Rhombohedral	2 weeks	Prisms with sharp edges
9	Rhombohedral	3 weeks	Small rods
10	Rhombohedral	2 weeks	Rods
12	Hexagonal	2 weeks	Plates
14	Rhombohedral	2 weeks	Needles
18	Rhombohedral	2 weeks	Shower of small crystals
24*	Hexagonal	2 weeks	Small rods with six edges
26*	Rhombohedral	>2 months	Thick needle
38	Rhombohedral	1 month	Brittle needles
39*	Rhombohedral	2 weeks	Prisms with sharp edges
46	Rhombohedral	2 weeks	Small needles
47*	Rhombohedral	1 month	Prisms with sharp edges

* Crystals grown under these conditions have more perfect optical appearance.

complete to about 2.6 Å resolution with an *R* factor of 8.8% for the shell between 2.6 and 3.0 Å resolution. For reflections with higher resolution, the merge factor increases dramatically and data beyond 2.5 Å resolution should be considered unreliable.

The cell constants of the rhombohedral crystals are $a = b = 42.38$ and $c = 131.70$ Å. The crystal-to-detector distance was 100 mm and a total of 130 frames with a frame size of 1.0° were collected. The resulting 38 834 reflections were merged to 5753 unique reflections with an overall merge factor of 12% (all data up to 1.3 Å resolution). At the onset of data collection with the rhombohedral crystal, reflections of up to 1.3 Å resolution were detected. During data collection, some decay occurred and the nominal resolution of the collected data is thus about 1.8 Å. However, rapid data collection on a synchrotron source or shock freezing the crystals can be expected to provide data of almost atomic resolution. Even in combination with a standard rotating-anode source, the rhombohedral crystal form of r(CCCCGGGG) constitutes one of the best diffracting RNA crystals reported to date.

For the hexagonal form, the assumption of a single octamer strand constituting the asymmetric unit would result in a volume per base pair of 1668 Å³. This value lies slightly above the average space requirement of 1480 Å³ (standard deviation ± 149 Å³) per base pair in 53 A-DNA crystal structures. Thus, the double helix would adopt crystallographic twofold symmetry and would be located on one of the two distinct twofold rotation axes present in the enantiomorphic space-group pair *P*6₁22/*P*6₅22. Such an arrangement is consistent with the self-rotation function [program *POLARRFN*, Version 2.6 (Collaborative Computational Project, Number 4, 1994); 10–3 Å resolution data, 10 Å integration radius, section $\kappa = 180^\circ$] for the hexagonal form which shows absence of non-crystallographic twofold rotation axes, providing evidence against a general positioning of the duplex. General rotation/translation function searches with program *AMoRe* (Collaborative Computational Project, Number 4, 1994; Navaza, 1994) using several A-form and A'-form models in space groups *P*6₁22 and *P*6₁ resulted in some solutions where molecular and crystallographic (normal to the unit-cell axes) twofold rotation axes coincided. The solutions with the highest correlation factors and lowest *R* factors generally resulted from searches with the tetragonal d(CCCCGGGG) A-DNA model

(Haran *et al.*, 1987) and a corresponding model with inserted 2'-hydroxyl groups. All searches in the enantiomorphic space groups $P6_522$ and $P6_5$ produced arrangements with deviating orientations of molecular twofold and crystallographic twofold axes. Moreover, the resulting packings in these space groups created unfavorable contacts and occasionally overlaps between neighboring duplexes, while the results of searches with favorable figures of merit in the space groups with right-handed sixfold screw axes showed no problematic lattice contacts. However, there was generally no clear discrimination between the best solution and those ranked lower, and the top solutions in various searches normally exhibited R factors that were quite high and never below 56% (including 25–5 Å resolution data). Despite the fact that the determined location of the duplex and the reasonable lattice provided evidence for the significance of the solution, we used an alternative search method in order to support its correctness. Selected A-type models were rotated and translated along the two distinct twofold rotation axes in space groups $P6_122$ and $P6_522$, using angle and shift increments of 10° and 0.05 (fractional), respectively. The best solution resulting from these searches was found to be nearly identical with the one established in the general search with the program *AMoRe*. The center of gravity of the duplex is thus located at -24 Å along the twofold rotation axis running perpendicular to the crystallographic x axis at $z = 0.25$ and its major groove opens towards the origin.

This solution was then subjected to Konnerth–Hendrickson type constraint least-squares refinement as modified for nucleic

acids (Quigley, Teeter & Rich, 1978) in space group $P6_122$, using a complete duplex and averaging the two strands after several cycles of refinement. Including data between 10 and 3 Å resolution, the R factor converged at 36% with some deviations from ideality in the backbone. The coordinates were further refined in space group $P6_1$ with program *X-PLOR* (Version 3.0, Brünger, Kuriyan & Karplus, 1987) and conventional refinement lowered the R factor to 34%. Simulated annealing was then performed between 3000 and 300 K in 25 K steps with 50 steps of 0.5 fs dynamics. Although the space group is $P6_122$, refinement in *X-PLOR* was carried out in $P6_1$ in order to maintain *via* NOE restraints a reasonable relative orientation of the two symmetry-related strands forming the duplex. Relative positions of guanine and cytosine bases in each base pair were restrained with three hydrogen bonds, and the two strands were restricted to their average position by means of the NCS-restraints-statement. The R factor dropped to 27% and the current R factor at 3 Å resolution after individual B factor refinement is 24%. Bond lengths and angles in the duplex display only minor deviations from ideality and the two strands adopt nearly perfect twofold symmetry. Moreover, electron-density maps show the duplex surrounded by continuous density. In the crystal lattice duplexes are stacked in a 3',3'/5',5'-fashion with almost ideal stacking interactions between terminal base pairs. Further refinement with incorporation of solvent molecules as well as data collection with crystals obtained under alternative conditions is in progress.

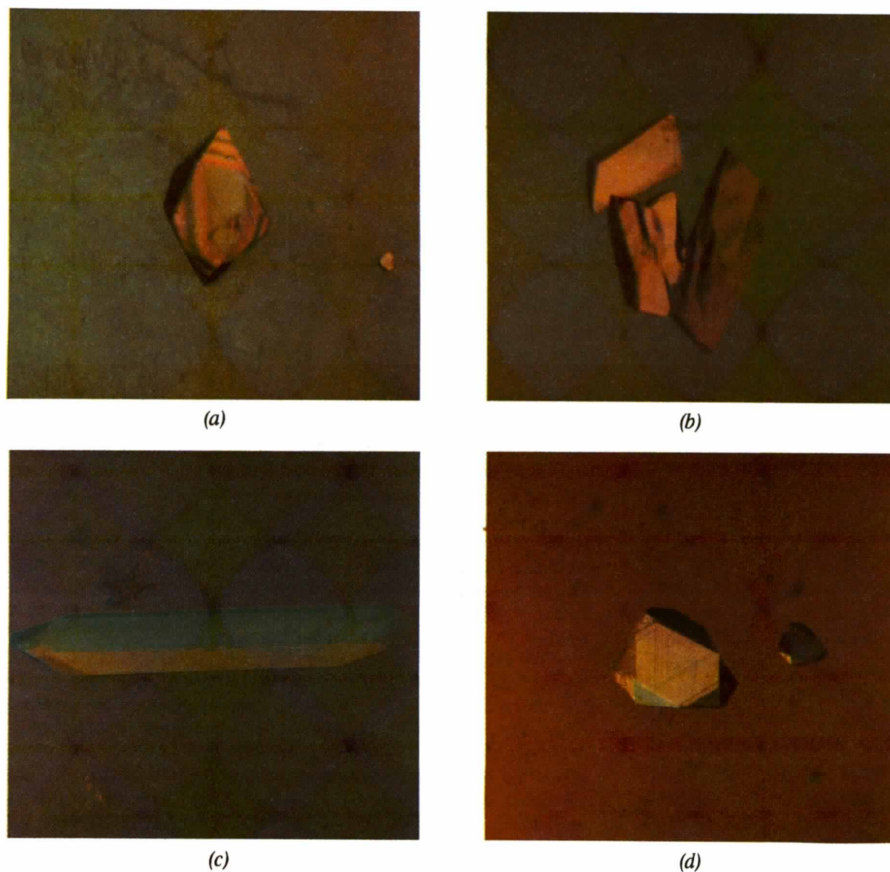


Fig. 1. Micrographs of hexagonal and rhombohedral crystal forms. (a) Modified condition 1; hexagonal form. (b) Condition 4; rhombohedral form. (c) Condition 26; rhombohedral form. (d) Condition 47; rhombohedral form.

Rhombohedral data (10–1.8 Å) were initially merged in Laue groups $\bar{3}$ and $\bar{3}m$, whereby the merging factor in $\bar{3}m$ was 0.6% lower (5.6 versus 5.0%). Moreover, a self-rotation function calculated in space group $R3$ indicated six non-crystallographic twofold rotation axes in the xy plane, running along the directions of the cell axes and their diagonal, as well as approximately perpendicular to these three directions (Fig. 2). An additional non-crystallographic twofold rotation axis runs parallel to the crystallographic threefold axis. All these findings pointed to space group $R32$ which differs from $R3$ by additional twofold rotation axes along the x and y axes and their diagonal. Thus, the above non-crystallographic twofolds, lying more or less perpendicular to the crystallographic ones as well as parallel to the z axis, would coincide with either the molecular twofold of the RNA duplex or intermolecular ones between duplexes. A rotation/translation search in space group $R3$ is complicated by the fact that one has to determine the orientations and positions of two independent duplexes (the calculated volume per base pair for 18 duplexes is 1424 Å³ and thus within the range associated with crystal structures of A-type oligonucleotide duplexes). Searching in space group $R32$, under the assumption of one duplex in a general position, would greatly facilitate structure determination. Alternatively, two independent duplexes, both adopting crystallographic twofold symmetry, could contribute one strand each to the asymmetric unit. In space group $R32$ there are two families of crystallographic twofold rotation axes which run parallel to one another, but are separated by 1/6 in the direction of the z axis. For obvious reasons, the two duplexes could not lie on the same twofold, but a situation whereby the duplexes were placed on each of the crystallographically distinct twofolds could not be rejected *a priori*.

Consequently, rotation and translation searches were performed with the program *AMoRe* in space group $R32$, initially anticipating one duplex in a general position. From Patterson maps it was concluded that the helix axis of either this one duplex or the axes of two duplexes had to be roughly parallel to the crystallographic threefold (Fig. 3). This observation alone was sufficient to rule out stacking of terminal base pairs of one duplex into the minor groove of a neighboring one, a packing mode found in almost all crystals of A-type DNA oligonucleotides. An interaction mode whereby duplexes would be stacked on top of one another, similar to the situation in the hexagonal form, seemed very likely. Rotational searches with the refined hexagonal structure as the model produced a number of solutions with relatively high correlation coefficients of around 60% which were consistent with the non-crystallographic twofold symmetries from the self-rotation function. However, the solutions from translational searches all led to overlaps between one or two terminal base pairs of adjacent duplexes and the R factors were generally quite high. At this point, one could trust the rotational solution to a certain extent, but the positioning of the duplex was clearly wrong. We felt that there was a good chance that the correct solution would be one which resulted in stacking interactions at both ends of the duplex. Therefore, the duplex was rotated and shifted manually, while simultaneously generating its symmetry mates in space group $R32$, until the resulting packing arrangement showed reasonable stacking for both terminal base pairs. The actual existence of such an arrangement with no obvious bad lattice contacts provided strong evidence for its correctness. Indeed, rigid-body refinement of the duplex placed in the above manner with the program *AMoRe* (Collaborative Computational Project, Number 4, 1994) led to an R factor of 44% with a

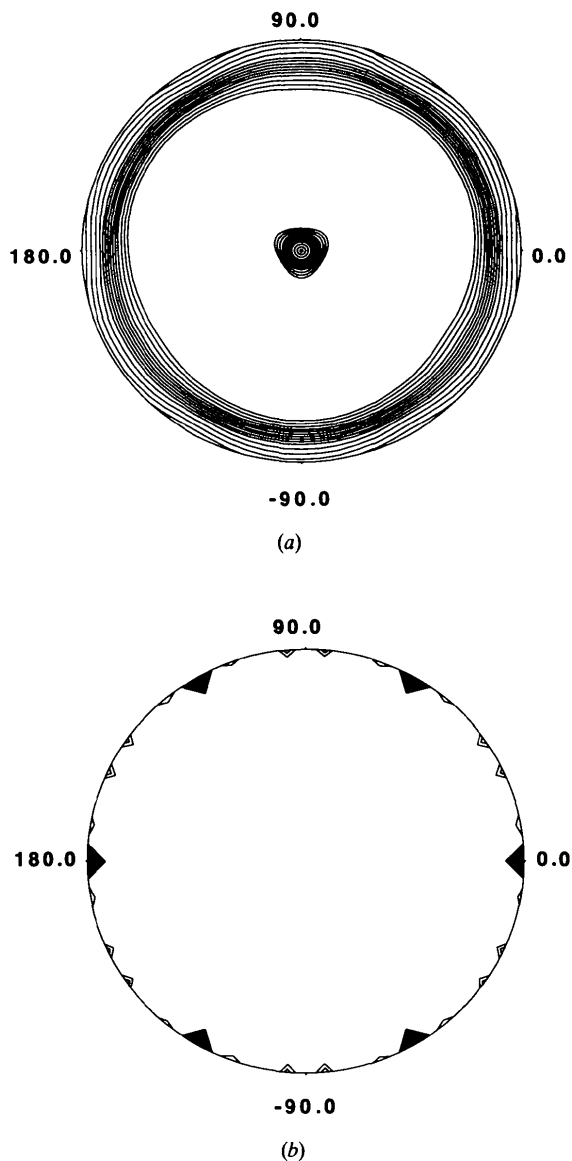


Fig. 2. Self-rotation function for the rhombohedral crystal form [program *POLARRFN* (Collaborative Computational Project, Number 4, 1994)]. (a) Section $\kappa = 180^\circ$ with a 10 Å integration radius. (b) Section $\kappa = 180^\circ$ with a 30 Å integration radius. Data between 15 and 3 Å were used in both cases and numbers in the drawings are values for angle φ . Thus, the crystallographic x axis runs along the horizontal ($\varphi = 0^\circ$), the crystallographic y axis is at $\varphi = 120^\circ$, and the z axis is then perpendicular to the plane of projection. Shorter integration radii with consequent inclusion of mostly intramolecular vectors result in smearing of equatorial peaks. The continuous band in (a) is the result of the superpositioning of crystallographic twofold rotation axes and non-crystallographic global intramolecular, local intramolecular as well as intermolecular twofold rotation axes. Larger integration radii expose the crystallographic twofolds as the strongest peaks (b, $\varphi = 0, 60^\circ$, etc.), with the non-crystallographic global intramolecular twofolds deviating by less than 10° (b, small peaks above and below the $\varphi = 0$ peak, plus symmetry-related ones). The remaining small peaks in (b) as well as the central peak in (a) are most likely a consequence of the crystallographic twofolds and the non-crystallographic molecular twofolds.

high correlation coefficient of 71% (including data between 10 and 3 Å). This solution was then refined with program *X-PLOR* to a current *R* factor of 26% including all data with $F \geq 2\sigma(F)$ between 10 and 1.8 Å resolution. Placement of solvent molecules and further refinement is under way.

The hexagonal and rhombohedral crystal forms of r(CCCCGGGG) thus belong to the class of oligonucleotide crystal structures with extensive stacking interactions between terminal base pairs in the lattice. Although very unusual for A-type DNA duplexes, such an interaction mode is rather common with crystal structures of B-DNA fragments or intercalator-DNA complexes. For example, in the crystal structure of a complex between a B-DNA hexamer and the anthracycline antibiotic nogalamycin (Egli, Williams, Frederick & Rich, 1991), DNA duplexes are stacked in a 3',3'/5',5' fashion, similar to the arrangement found in the hexagonal r(CCCCGGGG) form. For a comparison, the exclusive interaction mode between left-handed Z-DNA hexamers in the crystal is stacking of the 5',3'/5',3'-type between terminal base pairs. This generates infinite double helices with gaps due to the lack of phosphate groups between the terminal nucleotides, much like the ones found in the rhombohedral r(CCCCGGGG) form. It will be interesting to analyze the conformational changes of the RNA duplex as a consequence of the different environments in the hexagonal and rhombohedral crystal forms, but also with respect to other RNA's as well as to its related A-DNA with identical sequence. All A-DNA fragments except for a DNA tetramer (Conner, Yoon, Dickerson & Dickerson, 1984) feature a packing mode whereby terminal base pairs are stacked into the minor groove of adjacent duplexes with each duplex consequently contacting four neighbors. In contrast, in six of the seven crystal structures of RNA duplexes published to date (including the two presented here; the exception being the original 14-mer (Dock-Bregeon *et al.*, 1988)), molecules are stacked in an end-to-end fashion. Thus, the crystal packing modes of A-DNA and A-RNA double helices seem to be fundamentally different.

Outlook

Chemical synthesis can provide RNA oligonucleotides suitable for crystallographic experiments, and is probably the method of choice for the production of RNA fragments of up to around 20 nucleotides in milligram quantities. An additional benefit of chemical synthesis compared with

enzymatic RNA production is the possibility to incorporate various alternative synthons into oligonucleotides and hence generation of chimeric strands (*e.g.* Egli, Usman, Zhang & Rich, 1992; Usman & Cedergren, 1992; Lubini, Zürcher & Egli, 1994). Oligonucleotides have only rarely been shown to crystallize in different crystal systems or space groups (Shakked *et al.*, 1989; Jain & Sundaralingam, 1989). Possible reasons are the fact that in many cases only limited crystallization conditions were screened, or that once crystals suitable for diffraction experiments were obtained, the search for alternative conditions was abandoned. The existence of two different crystal forms of the same fragment, as in the case of the RNA octamer r(CCCCGGGG) reported here, offers the opportunity to analyze a RNA duplex in a fashion hitherto unavailable. Thus, the conformational flexibility of the RNA duplex and its dependence on the crystal environment can be assessed. Moreover, the detailed geometries of an A-DNA duplex and an A-RNA duplex with identical sequence can now be related. Preliminary crystallization trials have also resulted in growth of rhombohedral crystals under the reported conditions, but supplemented with various concentrations of earth alkali and transition metal ions. Data collection at a synchrotron source with the rhombohedral crystal form may provide a very high resolution structure of a RNA duplex, possibly revealing details of hydration and ion coordination thus far inaccessible.

We thank Dr Fritz K. Winkler of F. Hoffmann-LaRoche Ltd, Basel, for generous help with data collection and reduction. SP was supported by an ETH graduate fellowship.

References

- BAEYENS, K. J., DE BONDT, H. L. & HOLBROOK, S. R. (1995). *Nature Struct. Biol.* **2**, 56–62.
- BIOU, V., YAREMCHUK, A., TUKALO, M. & CUSACK, S. (1994). *Science*, **263**, 1404–1410.
- BRÜNGER, A. T., KURIYAN, J. & KARPLUS, M. (1987). *Science*, **235**, 458–460.
- COLLABORATIVE COMPUTATIONAL PROJECT, NUMBER 4 (1994). *Acta Cryst.* **D50**, 760–763.
- CONNER, B. N., YOON, C., DICKERSON, J. L. & DICKERSON, R. E. (1984). *J. Mol. Biol.* **174**, 663–695.
- CRUSE, W. B. T., SALUDJIAN, P., BIALA, E., STRAZEWSKI, P., PRANGÉ, T. & KENNARD, O. (1994). *Proc. Natl Acad. Sci. USA*, **91**, 4160–4164.
- DICKERSON, R. E. (1992). *Methods Enzymol.* **211**, 67–111.
- DOCK-BREGEON, A. C., CHEVRIER, B., PODJARNY, D., MORAS, D., DEBEAR, J. S., GOUGH, G. R., GILHAM, P. T. & JOHNSON, J. E. (1988). *Nature (London)*, **335**, 375–378.
- EGLI, M. (1994). *Structure Correlation*, edited by H.-B. BURGI & J. D. DUNITZ, pp. 705–749. New York: VCH.
- EGLI, M., USMAN, N., ZHANG, S. & RICH, A. (1992). *Proc. Natl Acad. Sci. USA*, **89**, 534–538.
- EGLI, M., WILLIAMS, L. D., FREDERICK, C. A. & RICH, A. (1991). *Biochemistry*, **30**, 1364–1372.
- FISHER, A. J. & JOHNSON, J. E. (1993). *Nature (London)*, **361**, 176–179.
- HARAN, T. E., SHAKKED, Z., WANG, A. H.-J. & RICH, A. (1987). *J. Biomol. Struct. Dynam.* **5**, 199–217.
- HOLBROOK, S. R., CHEONG, C., TINOCO JR, I. & KIM, S.-H. (1991). *Nature (London)*, **353**, 579–581.
- JAIN, S. & SUNDARALINGAM, M. J. (1989). *J. Biol. Chem.* **264**, 12780–12784.
- JANCARIK, J. & KIM, S.-H. (1991). *J. Appl. Cryst.* **24**, 409–411.
- JOSHUA-TOR, L. & SUSSMAN, J. L. (1993). *Curr. Opin. Struct. Biol.* **3**, 323–335.
- KENNARD, O. & HUNTER, W. N. (1991). *Angew. Chem. Int. Ed. Engl.* **30**, 1254–1277.
- KIM, S.-H., QUIGLEY, G. J., SUDDATH, F. L., MCPHERSON, A., SNEDEN, D., KIM, J. J., WEINZIERL, J. & RICH, A. (1973). *Science*, **179**, 285–288.

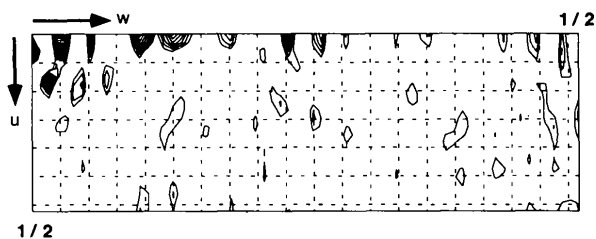


Fig. 3. Sharpened origin-removed Patterson function [$u0w$ section, E2OR-option, program *FFT* (Collaborative Computational Project, Number 4, 1994)] for the rhombohedral crystal form using 15–3 Å data. The grid is 3.4 Å and only a fourth of the section has been plotted (rest symmetry-equivalent). The map features more or less continuous stacking along the crystallographic threefold axis, indicating an orientation of the duplexes, whereby helix axes are nearly coaxially arranged and parallel to the *z* axis.

- LARSON, S. B., KOSZELAK, S., DAY, J., GREENWOOD, A., DODDS, J. A. & McPHERSON, A. (1993). *Nature (London)*, **61**, 179–182.
- LEONARD, G. A., MCAULEY-HECHT, K. E., EBEL, S., LOUGH, D. M., BROWN, T. & HUNTER, W. N. (1994). *Structure*, **2**, 483–494.
- LORENZ, S., FURSTE, J. P., BALD, R., ZHANG, M., RADERSCHALL, E., BETZEL, C., DAUTER, Z., WILSON, K. S. & ERDMANN, V. A. (1993). *Acta Cryst.* **D49**, 418–420.
- LUBINI, P., ZÜRCHER, W. & EGLI, M. (1994). *Chem. Biol.* **1**, 39–45.
- MORAS, D., COMAROMOND, M. B., FISCHER, J., WEISS, R., THIERRY, J. C., EBEL, J. P. & GIEGÉ, R. (1980). *Nature (London)*, **288**, 669–674.
- NAVAZA, J. (1994). *Acta Cryst.* **A50**, 157–163.
- OUBRIDGE, C., ITO, N., EVANS, P. R., TEO, C.-H. & NAGAI, K. (1994). *Nature (London)*, **372**, 432–438.
- PLEY, H. W., FLAHERTY, K. M. & MCKAY, D. B. (1994). *Nature (London)*, **372**, 68–74.
- QUIGLEY, G. J., TEETER, M. M. & RICH, A. (1978). *Proc. Natl Acad. Sci. USA*, **75**, 64–68.
- RABINOVICH, D., HARAN, T., EISENSTEIN, M. & SHAKKED, Z. (1988). *J. Mol. Biol.* **200**, 151–161.
- ROBERTUS, J. D., LADNER, J. E., FINCH, J. T., RHODES, D., BROWN, R. S., CLARK, B. F. C. & KLUG, A. (1974). *Nature (London)*, **250**, 546–551.
- ROULD, M. A., PERONA, J. J., SOLL, D. & STEITZ, T. A. (1989). *Science*, **246**, 1135–1142.
- RUFF, M., KRISHNASWAMY, S., BOEGLIN, M., POTERSZMAN, A., MITSCHLER, A., PODJARNY, A., REES, B., THIERRY, J. C. & MORAS, D. (1991). *Science*, **252**, 1682–1689.
- SCARINGE, S. A., FRANCKLYN, C. & USMAN, N. (1990). *Nucleic Acids Res.* **18**, 5433–5441.
- SHAKKED, Z., GUERSTEIN-GUZIKEVICH, G., EISENSTEIN, M., FROLOW, F. & RABINOVICH, D. (1989). *Nature (London)*, **342**, 456–460.
- USMAN, N. & CEDERGREN, R. (1992). *Trends Biochem. Sci.* **17**, 334–339.
- USMAN, N., EGLI, M. & RICH, A. (1992). *Nucleic Acids Res.* **20**, 6695–6699.
- VALEGÅRD, K., MURRAY, J. B., STOCKLEY, P. G., STONEHOUSE, N. J. & LILJAS, L. (1994). *Nature (London)*, **371**, 623–626.
- WINCOTT, F. W., DiRENZO, A., TRACZ, D., SHAFFER, C., GRIMM, S., WORKMAN, C., SWEEDLER, D. & USMAN, N. (1995). *Nucleic Acids Res.*